

Visual-textual Capsule Routing for Text-based Video Segmentation

Bruce McIntosh

bwmcint@gmail.com

Kevin Duarte

kevin95duarte@gmail.com

Yogesh S Rawat

yogesh@crcv.ucf.edu

Mubarak Shah

shah@crcv.ucf.edu

Center for Research in Computer Vision
University of Central Florida
Orlando, FL, 32816

Abstract

Joint understanding of vision and natural language is a challenging problem with a wide range of applications in artificial intelligence. In this work, we focus on integration of video and text for the task of actor and action video segmentation from a sentence. We propose a capsule-based approach which performs pixel-level localization based on a natural language query describing the actor of interest. We encode both the video and textual input in the form of capsules, which provide a more effective representation in comparison with standard convolution based features. Our novel visual-textual routing mechanism allows for the fusion of video and text capsules to successfully localize the actor and action. The existing works on actor-action localization are mainly focused on localization in a **single** frame instead of the full video. Different from existing works, we propose to perform the localization on **all** frames of the video. To validate the potential of the proposed network for actor and action video localization, we extend an existing actor-action dataset (A2D) with annotations for all the frames. The experimental evaluation demonstrates the effectiveness of our capsule network for text selective actor and action localization in videos. The proposed method also improves upon the performance of the existing state-of-the-art works on single frame-based localization.

1. Introduction

Deep learning and artificial neural networks have led to outstanding advancements in the fields of computer vision and natural language processing (NLP). In recent years, the vision and NLP communities have proposed several tasks which require methods to understand both visual and textual inputs. These include visual question answering [1], image and video captioning [29, 30], visual text correction [21], and video generation from text inputs [18]. In this work, we focus on detection of actors and actions in a video through

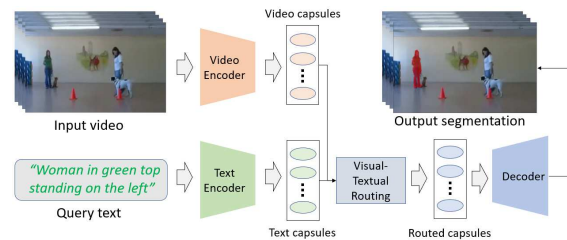


Figure 1. Overview of the proposed approach. For a given video, we want to localize the actor and action which are described by an input textual query. Capsules are extracted from both the video and the textual query, and a joint EM routing algorithm creates high level capsules, which are further used for localization of selected actors and actions.

natural language queries.

Actor and action detection in a video is an important task in computer vision and it has many applications, such as video retrieval, human-machine interaction, and surveillance. Most of the existing methods focus on detection of actor/action which are from a fixed set of categories. Instead of having these fixed categories, one can leverage natural language to describe the actors and actions which needs to be localized. This describes the task of actor and action video segmentation from a sentence [8]: given a video and a natural language sentence input, the goal is to output a pixel-level localization of the actor described by the sentence. For a method to perform this task, it must effectively merge the visual and textual inputs to generate a segmentation mask for the actor of interest.

The existing methods for video encoding are mainly based on 3D convolutions. The availability of large-scale datasets allow us to train effective 3D convolution based models, however, this encoded representation has some limitations as it fails to capture the relationship between different features. Capsule-based networks address some of these limitations and are effective in modeling visual entities and capturing their relationships [24]. Capsule net-

works are composed of groups of neurons called capsules which model objects or object-parts. These capsules undergo a routing-by-agreement procedure which allows it to learn relationships between these entities. Capsule networks are shown to be effective in both video [5] as well as textual domain [31]. In this work, we explore the use of capsules to jointly encode and merge visual and textual information for the task of actor and action detection in videos.

We propose an end-to-end capsule-based network for actor-action segmentation using a natural language query. The video and the textual query, both are encoded as capsules for learning an effective representation. We demonstrate that capsules and routing-by-agreement can be utilized for the integration of both visual and textual information. Our novel routing algorithm finds agreement between the visual and textual entities to produce a unified representation in the form of visual-textual capsules.

Our main contributions are summarized as follows:

- We propose an end-to-end capsule network for the task of selective actor and action localization in videos, which encodes both the video and the textual query in the form of capsules.
- We introduce a novel visual-textual capsule routing algorithm which fuses both modalities to create a unified capsule representation.
- To demonstrate the potential of the proposed text selective actor and action localization in videos, we extend the annotations in A2D dataset to full video clips.

Our experiments demonstrate the effectiveness of the proposed method, and we show its advantage over existing state-of-the-art works both qualitatively and quantitatively.

2. Related Work

Vision and Language Both vision and language have been used in several challenging problems. Several works have dealt with image captioning [7, 27] and video captioning [6] where a natural language description is generated for a given image or video. Zero-shot object detection from a textual input is explored by [20], which can localize novel object instances when given a textual description. In the video domain, a popular problem is that of temporal localization using natural language [9, 3, 4], where a method must localize the temporal boundary of the action described by a text query. The task of actor and action video segmentation given a sentence is similar, but a pixel-level segmentation of the described actor is output. The only work dealing with this is [8], however only a single frame is segmented. We believe that video segmentation should produce a segmentation for *all frames* in a video, so we extend the A2D dataset with annotations for all frames.

Merging Visual and Textual Inputs Hu *et al.* [12] introduced the problem of segmenting images based on a natural language expression; their method for merging images and text in a convolutional neural network (CNN) was by concatenating features extracted from both modalities and performing a convolution to obtain a unified representation. [19] propose a different approach to merge these modalities for the task of tracking a target in a video; they use an element-wise multiplication between the image features and the sentence features in a process called dynamic filtering. These are the two most commonly used approaches for merging both vision and language in a neural network. We present the first capsule-based approach which uses routing-by-agreement to merge both visual and textual inputs.

Capsule Networks Hinton *et al.* first introduced the idea of capsules in [10], and subsequently capsules were popularized in [24], where dynamic routing for capsules was proposed. This was further extended in [11], where a more effective EM routing algorithm was introduced. Recently, capsule networks have shown state-of-the-art results for human action localization in video [5], object segmentation in medical images [17], and text classification [31]. [32] proposed a capsule-based attention mechanism for the task of visual question answering. To our knowledge, our work is the first to use capsules and routing to combine both video and natural language inputs.

3. Visual-Textual Capsule Routing

Brief Introduction to Capsule Networks A capsule is a group of neurons that models objects, or parts of objects. In this work, we use the matrix capsule formulation proposed by [11], where a capsule, C , is composed of a 4×4 pose matrix M , and an activation $a \in [0, 1]$. The pose matrix contains the instantiation parameters, or properties, of the object modeled by the capsule and the activation is the existence probability of the object. Capsules from one layer pass information to capsules through a routing-by-agreement operation. This begins when the lower level capsules produce votes for the capsules in the higher level; these votes, $V_{ij} = M_i T_{ij}$, are the result of a matrix multiplication between learned transformation matrices, T_{ij} , and the lower level pose matrices, where i and j are the indices of the lower and higher level capsules respectively. Once these votes are obtained, they are used in the EM-routing algorithm to obtain the higher level capsules C_j , with pose matrices M_j and activations a_j .

Our Routing Method Capsules represent entities and routing uses *high-dimensional coincidence filtering* [11] to learn part-to-whole relationships between these entities. We argue that this allows capsule networks to effectively merge

visual and textual information. There are several possible ways to implement this using capsule networks. One simple approach would be to apply a convolutional method (concatenation followed by a 1x1 convolution [12] or multiplication/dynamic filtering [19]) to create a unified representation in the form of feature maps, and extract a set of capsules from these feature maps. This, however, would not perform much better than the fully convolutional networks, since the same representation is obtained from the merging of the visual and textual modalities, and the only difference is how they are transformed into segmentation maps.

Another method would be to first extract a set of capsules from the video, and then apply the dynamic filtering on these capsules. This can be done by (1) applying a dynamic filter to the pose matrices of the capsules, or (2) applying a dynamic filter to the activations of the capsules. The first is not much different than the simple approach described above, since the same feature map representation would be present in the capsule pose matrices, as opposed to the layer prior to the capsules. The second approach would just discount importance of the votes corresponding to entities not present in the sentence; this is not ideal, since it does not take advantage of routing’s ability to find agreement between entities in both modalities.

Instead, we propose an approach that leverages the fact that the same entities exist in both the video and sentence inputs and that routing can find similarities between these entities. Our method allows the network to learn a set of entities (capsules) from both the visual and sentence inputs. With these entities, the capsule routing finds the similarity between the objects in the video and sentence inputs to generate a unified visual-textual capsule representation.

More formally, we extract a grid of capsules describing the visual entities, C_v , with pose matrices M_v and activations a_v from the video. Similarly, we generate sentence capsules, C_s , with pose matrices M_s and activations a_s for the sentence. Each set of capsules has learned transformation matrices T_{vj} and T_{sj} , for video and text respectively, which are used to cast votes for the capsules in the following layer. Video capsules at different spatial locations share the same transformation matrices. Using the procedure described in Algorithm 1, we obtain a grid of higher-level capsules, C_j . This algorithm allows the network to find similarity, or agreement, between the votes of the video and sentence capsules at every location on the grid. If there is agreement, then the same entity exists in both the sentence and the given location in the video, leading to a high activation of the capsule corresponding to that entity. Conversely, if the sentence does not describe the entity present at the given spatial location, then the activation of the higher-level capsules will be low since the votes would disagree.

Algorithm 1 *Visual-Textual Capsule Routing*. The inputs to this procedure are the video capsules’ poses and activations (M_v, a_v) and the sentence capsules’ poses and activations (M_s, a_s). The $\{\bullet; \bullet\}$ operation is concatenation, such that the activations and votes the video and sentence capsules are inputs to the EM ROUTING procedure described in [11].

```

1: procedure VTRROUTING( $M_v, a_v, M_s, a_s$ )
2:    $V_{sj} \leftarrow M_s T_{sj}$ 
3:   for  $x = 1$  to  $W$  do
4:     for  $y = 1$  to  $H$  do
5:        $V_{vj} \leftarrow M_v[x, y] T_{vj}$ 
6:        $a \leftarrow \{a_s; a_v[x, y]\}$ 
7:        $V \leftarrow \{V_{sj}; V_{vj}\}$ 
8:        $C_j[x, y] \leftarrow \text{EM ROUTING}(a, V)$ 
9:   return  $C_j$ 

```

4. Network Architecture

The overall network architecture is shown in Figure 2. In this section, we discuss the components of the architecture as well as the objective function used to train the network.

4.1. Video Capsules

The video input consists of $4 \times 224 \times 224$ frames. The process for generating video capsules begins with a 3D convolutional network known as I3D [2], which generates $832 \times 28 \times 28$ spatio-temporal feature maps taken from the maxpool3d_3a_3x3 layer. Capsule pose matrices and activations are generated by applying a 9×9 convolution operation to these feature maps, with linear and sigmoid activations respectively. Since there is no padding for this operation, the result is a 20×20 capsule layer with 8 capsule types.

4.2. Sentence Capsules

A series of convolutional and fully connected layers is used to generate the sentence capsules. First, each word from the sentence is converted into a size 300 vector using a word2vec model pre-trained on the Google News Corpus [22]. The sentence representation is then passed through 3 parallel stages of 1D convolution with kernel sizes of 2, 3 and 4 with a ReLU activation. We then apply max-pooling to obtain 3 vectors, which are concatenated and passed through a max-pooling layer to obtain a single length 300 vector to describe the entire sentence. A fully connected layer then generates the 8 pose matrices and 8 activations for the capsules which represent the entire sentence. We found that this method of generating sentence capsules performed best in our network: various other methods are explored in the Supplementary Material.

4.3. Merging and Masking

Once the video and sentence capsules are obtained, we merge them using the proposed routing algorithm. The re-

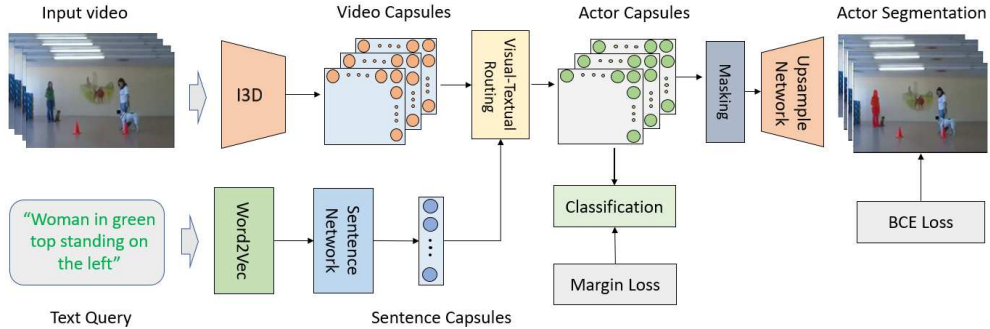


Figure 2. Network Architecture. Capsules containing spatio-temporal features are created from video frames, and capsules representing a textual query are created from natural language sentences. These capsules are routed together to create capsules representing actors in the image. The visual-textual capsule poses go through a masking procedure and an upsampling network to create binary segmentation masks of the actor specified in the query.

result of the routing operation is a 20×20 grid with 8 capsule types - one for each actor class in the A2D dataset and one for a “background” class, which is used to route unnecessary information. The activations of these capsules correspond to the existence of the corresponding actor at the given location, so averaging the activations over all locations gives us a classification prediction over the video clip. We find that this class to capsule correspondence improves the network’s segmentations overall.

We perform the capsule masking as described in [24]. When training the network, we mask (multiply by 0) all pose matrices not corresponding to the ground truth class. At test time, we mask the pose matrices not corresponding to the predicted class. These masked poses are then fed into an upsampling network to generate a foreground/background actor segmentation mask. Our network outperforms contemporary methods without classification and masking, but this extra supervision signal improves the performance. We explore this further in our ablations.

4.4. Upsampling Network

The upsampling network consists of 5 convolutional transpose layers. The first of these increases the feature map dimension from 20×20 to 28×28 with a 9×9 kernel, which corresponds to the 9×9 kernel used to create the video capsules from the I3D feature maps. The following 3 layers have $3 \times 3 \times 3$ kernels and are strided in both time and space, so that the output dimensions are equal to the input video dimensions ($4 \times 224 \times 224$). The final segmentation is produced by a final layer which has a $3 \times 3 \times 3$ kernel. *Note that a unique feature of our method compared to previous method is it outputs segmentations for all input frames, rather than a single frame segmentation per video clip input.* We use parameterized skip connections from the I3D encoder to obtain more fine-grained segmentations.

4.5. Objective Function

The network is trained end-to-end using an objective function based on classification and segmentation. For classification, we use a spread loss which is computed as:

$$L_c = \sum_{i \neq t} \max(0, m - (a_t - a_i))^2, \quad (1)$$

where $m \in (0, 1)$ is a margin, a_i is the activation of the capsule corresponding to class i , and a_t is the activation of the capsule corresponding to the ground-truth class. During training, m is linearly increased between 0.2 and 0.9, following the standard set by [11, 5].

The segmentation loss is computed using sigmoid cross entropy. When averaged over all N pixels in the segmentation map, we get the following loss:

$$L_s = -\frac{1}{N} \sum_{j=1}^N p_j \log(\hat{p}_j) - (1 - p_j) \log(1 - \hat{p}_j), \quad (2)$$

where $p_j \in \{0, 1\}$ is the ground-truth segmentation map and $\hat{p}_j \in [0, 1]$ is the network’s output segmentation map.

The final loss is a weighted sum between the classification and segmentation losses:

$$L = \lambda L_c + (1 - \lambda) L_s, \quad (3)$$

where λ is set to 0.5 when training begins. Since the network quickly learns to classify the actor when given a sentence input, we set λ to 0 when the classification accuracy saturates (over 95% on the validation set). We find that this reduces over-fitting and results in better segmentations.

5. Experiments

Implementation Details The network was implemented using PyTorch [23]. The I3D used weights pretrained on Kinetics [14] and fine tuned on Charades [26]. The network was trained using the Adam optimizer [16] with a learning rate of .001. As video resolutions vary within different

	Overlap					mAP	IoU	
	P@0.5	P@0.6	P@0.7	P@0.8	P@0.9	0.5:0.95	Overall	Mean
Hu <i>et al.</i> [12]	34.8	23.6	13.3	3.3	0.1	13.2	47.4	35.0
Li <i>et al.</i> [19]	38.7	29.0	17.5	6.6	0.1	16.3	51.5	35.4
Gavrilyuk <i>et al.</i> [8]	50.0	37.6	23.1	9.4	0.4	21.5	55.1	42.6
Our Network	52.6	45.0	34.5	20.7	3.6	30.3	56.8	46.0

Table 1. Results on A2D dataset with sentences. Baselines [12, 19] take only single image/frame inputs. Gavrilyuk *et al.* [8] uses multi-frame RGB and Flow inputs. Our model uses only multi-frame RGB inputs and outperforms other state-of-art-methods in all metrics without the use of optical flow.

	Overlap					mAP	IoU	
	P@0.5	P@0.6	P@0.7	P@0.8	P@0.9	0.5:0.95	Overall	Mean
Hu <i>et al.</i> [12]	63.3	35.0	8.5	0.2	0.0	17.8	54.6	52.8
Li <i>et al.</i> [19]	57.8	33.5	10.3	0.6	0.0	17.3	52.9	49.1
Gavrilyuk <i>et al.</i> [8]	69.9	46.0	17.3	1.4	0.0	23.3	54.1	54.2
Our Network	67.7	51.3	28.3	5.1	0.0	26.1	53.5	55.0

Table 2. Results on JHMDB dataset with sentences. Our model outperforms other state-of-the-art methods at higher IoU thresholds and in the mean average precision metric.

datasets, all video inputs are scaled to 224×224 while maintaining aspect ratio through the use of horizontal black bars. When using bounding box annotations, we consider pixels within the bounding box to be foreground and pixels outside of the bounding box to be background.

5.1. Single-Frame Segmentation from a Sentence

In this experiment, a video clip and a sentence describing one of the actors in the video are taken as inputs, and the network generates a binary segmentation mask localizing the actor. Similar to previous methods, the network is trained and tested on the single frame annotations provided in the A2D dataset. To compare our method with previous approaches, we modify our network in these experiments. We replace the 3d convolutional transpose layers in our up-sampling network to 2d convolutional transpose layers to output a single frame segmentation.

Datasets We conduct our experiments on two datasets: A2D [28] and J-HMDB [13]. The A2D dataset contains 3782 videos (3036 for training and 746 for testing) consisting of 7 actor classes, 8 action classes, and an extra action label *none*, which accounts for actors in the background or actions different from the 8 action classes. Since actors cannot perform all labeled actions, there are a total of 43 valid actor-action pairs. Each video in A2D has 3 to 5 frames which are annotated with pixel-level actor-action segmentations. The J-HMDB dataset contains 928 short videos with 21 different action classes. All frames in the J-HMDB dataset are annotated with pixel-level segmentation masks. Gavrilyuk *et al.* [8] extended both of these datasets with human generated sentences that describe the actors of interest

for each video. These sentences use the actor and action as part of the description, but many do not include the action and rely on other descriptors such as location or color.

Evaluation We evaluate our results using all metrics used in [8]. The *overall IoU* is the intersection-over-union (IoU) over all samples, which tends to favor larger actors and objects. The *mean IoU* is the IoU averaged over all samples, which treats samples of different sizes equally. We also measure the precision at 5 IoU thresholds and the mean average precision over .50 : .05 : .95.

Results We compare our results on A2D with previous approaches in Table 1. Our network outperforms previous state-of-the-art methods in all metrics, and has a notable 8.8% improvement in the mAP metric, *even though we do not employ optical-flow*, which requires extra computation. We also find that our network achieves much stronger results at higher IoU thresholds, which signifies that the segmentations produced by the network are more fine-grained and adhere to the contours of the queried objects. Qualitative results on A2D can be found in Figure 3.

Following the testing procedure in [8], we test on all the videos of J-HMDB using our model trained on A2D without fine-tuning. The results on J-HMDB are found in Table 2; our network outperforms other methods at the higher IoU thresholds (0.6, 0.7, and 0.8), the mAP metric, and in mean IoU. We perform slightly worse at the lower threshold and in overall IoU. We find that our network performs poorly on J-HMDB actions which have little motion like “brush-hair”, “stand”, and “sit” (which have an IoU > 0.5 for less than 20% of the videos). On the other hand, our network

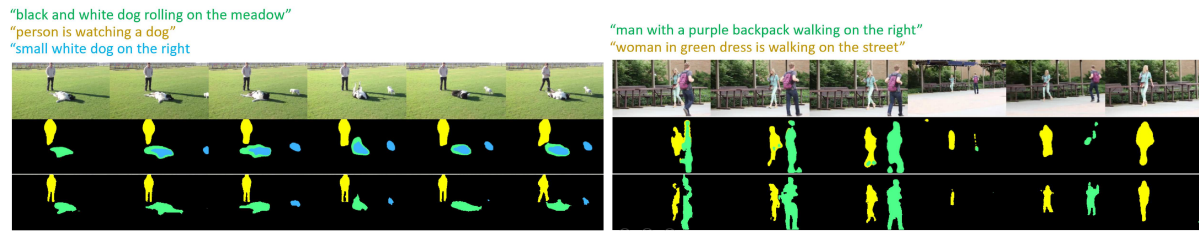


Figure 3. A comparison of our results with [8]. The sentence query colors correspond with the segmentation colors. The first row are frames from the input video. The second row shows the segmentation output from [8], and the third row shows the segmentation output from our model. In both examples, our model produces more finely detailed output, where the separation of the legs can be clearly seen. Our model also produces an output that is more accurately conditioned on the sentence query, as seen in the first example where our network segments the correct dog for each query, while [8] incorrectly selects the center dog for both queries.

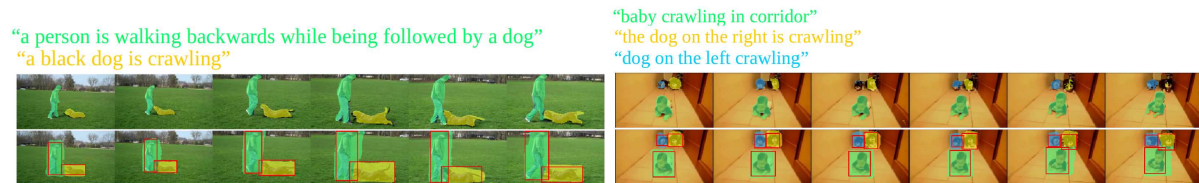


Figure 4. Qualitative results. The sentence query colors correspond with the segmentation colors. The first row contains the segmentations from the network trained only using pixel-wise annotations, and the second row contains the segmentations from the network trained using bounding box annotations on all frames. The segmentations from the network trained using bounding boxes are more box-like, but the extra training data leads to fewer missegmentations or under-segmentations as seen in the second example.

performs well on actions with larger amounts of motion like “pullup”, “swing baseball”, and “shoot ball”. Since A2D videos tend to have large amounts of motion, we believe that training on A2D forced our network to focus on motion cues which are not present in J-HMDB.

5.2. Full Video Segmentation from a Sentence

In this set of experiments, we train the network using the bounding box annotations for all the frames. Since previous baselines only output single frame segmentations, we test our method against our single-frame segmentation network as a baseline which can generate segmentations for an entire video, by processing the video frame-by-frame.

Importance of full video segmentation Previous methods for actor and action video segmentation from a sentence [8] process multiple frames but only segments a single frame at a time. We find this to be a weakness for two reasons: 1) it negatively impacts the temporal consistency of the generated segmentations and 2) it increases the computational time for generating segmentations for an entire video. Therefore, we propose a method which generates segmentation masks for the entire video at a time.

A2D dataset extension To successfully train and evaluate such a model, one would need a video dataset which contained localization annotations for all video frames. To this end, we extend the A2D dataset by adding bounding

box localizations for the actors of interest in every frame of the dataset. This allows us to train and test our method using the entire video, not just the 3 to 5 key frames which were previously annotated. The extended A2D dataset contains annotations for 6046 actors, with an average of 136 bounding boxes per actor. These annotations will be made publicly available.

Datasets For the full video segmentation experiments we use the extended A2D dataset. We use the same train and test video splits defined in [8], but the new annotations allow for training and evaluation on all video frames. The J-HMDB dataset has annotations on all frames, so we can evaluate the method on this dataset as well.

Evaluation To evaluate the segmentation results for entire videos, we consider each video as a single sample. Thus, the IoU computed is the intersection-over-union between the ground-truth tube and the generated segmentation tube. Using this metric, we can calculate the *video overall IoU* and the *video mean IoU*; the former will favor both larger objects and objects in longer videos, while the latter will treat all videos equally. We also measure the precision at 5 different IoU thresholds and the video mean average precision over .50 : .05 : .95.

Results Since the network is trained using the bounding box annotations, the segmentations are more block-like, but

	Video Overlap					v-mAP	Video IoU	
	P@0.5	P@0.6	P@0.7	P@0.8	P@0.9	0.5:0.95	Overall	Mean
Key frames (pixel)	9.6	1.6	0.4	0.0	0.0	1.8	34.4	26.6
Key frames (bbox)	41.9	33.3	22.2	10.0	0.1	21.2	51.5	41.3
All frames	45.6	37.4	25.3	10.0	0.4	23.3	55.7	41.8

Table 3. Results on A2D dataset with bounding box annotations. The first row is for the network trained with only pixel-level annotations on key frames of the video, and evaluated with its pixel-wise segmentation output. The second is the same network, but a bounding-box is placed around its segmentation output for evaluation. The final row, is the network trained with bounding box annotations on all frames.

it still successfully segments the actors described in the given queries. We compare the qualitative results between the network trained only using fine-grained segmentations and the network trained using bounding box annotations in Figure 4. When tested on the A2D dataset, we find that there is a significant improvement in all metrics when compared to the network trained only on single frames with pixel-wise segmentations. However, this is to be expected, since the ground-truth tubes are bounding boxes and box-like segmentations around the actor would produce higher IoU scores. For a fairer comparison, we place a bounding box around the fine-grained segmentations produced by the network trained on the pixel-wise annotations; this produces better results since the new outputs more resemble the ground-truth tubes. Even with this change, the network trained on bounding box annotations has the strongest results since it learned from all frames in the training videos, as opposed to a handful of frames per video (Table 3).

The J-HMDB dataset has pixel-level annotations for all frames, so the box-like segmentations produced by the network should be detrimental to results; we found that this was the case: the network performed poorly when compared to the network trained on fine-grained pixel-level annotations. However, if evaluation is performed on bounding boxes surrounding the ground-truth segmentations, then considerable improvements are observed across all metrics.

5.3. Image Segmentation Conditioned on Sentences

To investigate the versatility of the visual-textual routing algorithm, we also evaluate our method by segmenting images based on text queries. To make as few modifications to the network as possible, the single images are repeated to create a “boring” video input with 4 identical frames.

Dataset We use the ReferItGame dataset [15], which contains 20000 images with 130525 natural language expressions describing various objects in the images. We use the same train/test splits as [12, 25], with 9000 training and 10000 testing images. Unlike A2D there are no predefined set of actors, so no classification loss or masking is used.

Results We obtain similar results to other state-of-the-art approaches, even though our network architecture is de-

signed for actor/action video segmentation. At high IoU thresholds, our network’s precision outperforms [12] and is within 3% of [25]. This demonstrates that our proposed method for merging visual and textual information is effective on multiple visual modalities - both videos and images.

5.4. Ablation Studies

The ablation experiments were trained and evaluated using the pixel-level segmentations from the A2D dataset. All ablation results can be found in Table 4.

Classification and Masking We test the influence of the classification loss for this segmentation task, by running an experiment without back-propagating this loss. Without classification, the masking procedure would fail at test time, so masking is not used and all poses are passed forward to the upsampling network. This performed slightly worse than the baseline in all metrics, which shows that the classification loss and masking help the capsules learn meaningful representations. The network, however, still performs segmentation well without this extra supervision: this ablation outperforms previous methods on the A2D dataset in all metrics except Overlap P@0.5. To further investigate the effects of masking, we perform an experiment with no masking, but with the classification loss. Surprisingly, it performs worse than the network without masking nor classification loss; this signifies that classification loss can be detrimental to this segmentation task, if there is no masking to guide the flow of the segmentation loss gradient.

Effectiveness of Visual-Textual Routing We run several experiments to compare our visual-textual capsule routing procedure with alternative methods for merging video and text. We test the four other methods for fusing visual and textual information described earlier: the two trivial approaches (concatenation and multiplication), and the two methods which apply dynamic filtering to the video capsules (filtering the pose matrices and filtering the activations). The two trivial, convolutional-based approaches lead to a significant decrease in performance (a decrease of about 21% and 11% in mean IoU respectively) when compared to our visual-textual routing approach. Moreover, applying dynamic filtering to the video capsules results in about

	P@0.5	mAP	Mean IoU
No L_c nor Masking	49.4	28.8	43.6
No Masking (with L_c)	48.3	27.8	42.5
Concatenation	22.9	9.9	25.0
Multiplication	38.4	19.4	35.0
Filter Poses	49.1	29.1	42.7
Filter Activations	48.8	29.2	43.0
Our Network	52.6	30.3	46.0

Table 4. Ablations on the A2D dataset with sentences. The last row shows the results of our final network.

a 3% decrease in mean IoU and a 4% decrease in Overlap P@0.5, showing that it is not a simple task to extend techniques developed for CNNs, like dynamic filtering, to capsule networks. Rather, new capsule and routing based approaches, like visual-textual routing, must be developed to fully leverage the capabilities of capsule networks.

6. Discussion and Analysis

Failure Cases We find that the network has two main failure cases: (1) the network incorrectly selects an actor which is not described in the query, and (2) the network fails to segment anything in the video. Figure 6 contains examples of both cases. The first case occurs when the text query refers to an actor/action pair and multiple actors are doing this action or the video is cluttered with many possible actors from which to choose. This suggests that an improved video encoder which extracts better video feature representations and creates more meaningful video capsules could improve results. The second failure case tends to occur when the queried object is small, which is often the case with the “ball” class or when the actor of interest is far away.

How sentences are utilized We analyze the extent to which the model leverages the visual input and textual query. We present several cases where the network is given multiple queries for the same video in Figure 5. If the network is given a query which is invalid for a given video - this occurs when the actor described in the sentence is not present in the video - we find that our network correctly segments nothing; this behaviour is depicted in the first image of Figure 5. Moreover, if the network is given a sentence which describes multiple actors in the scene, it can segment all actors that are being described; this can be seen in the second image of Figure 5 where the sentence “Dogs running on the beach” is given to the network and both dogs are segmented. Our network can segment based on the action specified in the query; when given two similar sentences “The man walking to the right” and “The man standing on the right”, the network has learned the difference between the walking and standing actions and correctly segments the



Figure 5. These examples demonstrate the discriminative ability of the network. In the first image, the network correctly segments nothing when the query is not present within the video. The second image illustrates our network’s ability to segment multiple actors if they both fit the sentence’s description. The last two images show our network’s ability to discriminate based on the action.



Figure 6. Some failure cases. In the first two examples, the network chooses the wrong actor; in the second two, it is unable to find the queried actor due to their small size.

walking person only when the prior sentence is given. The A2D dataset is focused on actors and actions, so these tend to be the most powerful descriptors the network learns. The words “left” and “right” are frequently found in the training sentences, so the network seems to have a good grasp of these words as well. The network also understands other descriptors like color or size, but we find that these are less reliable since they occur less frequently in the training set.

7. Conclusion

In this work, we propose a capsule network for localization of actor and actions based on a textual query. The proposed framework makes use of capsules for both video as well as textual representation. By using visual-textual routing, our network successfully segments actors and actions in video, conditioned on a textual query. We extended the A2D dataset from single frame to all frame annotation to validate our performance. We demonstrate the effectiveness of visual-textual capsule routing and observe performance improvements over state-of-the art approaches.

Acknowledgments

This research is based upon work supported in parts by the National Science Foundation under Grants No. 1741431 and the Office of the Director of National Intelligence (ODNI), Intelligence Advanced Research Projects Activity (IARPA), via IARPA RD Contract No. D17PC00345. The views, findings, opinions, and conclusions or recommendations contained herein are those of the authors and should not be interpreted as necessarily representing the official policies or endorsements, either expressed or implied, of the NSF, ODNI, IARPA, or the U.S. Government. The U.S. Government is authorized to reproduce and distribute reprints for Governmental purposes notwithstanding any copyright annotation thereon.

References

- [1] Stanislaw Antol, Aishwarya Agrawal, Jiasen Lu, Margaret Mitchell, Dhruv Batra, C Lawrence Zitnick, and Devi Parikh. Vqa: Visual question answering. In *Proceedings of the IEEE international conference on computer vision*, pages 2425–2433, 2015.
- [2] Joao Carreira and Andrew Zisserman. Quo vadis, action recognition? a new model and the kinetics dataset. In *2017 IEEE Conference on Computer Vision and Pattern Recognition (CVPR)*, pages 4724–4733. IEEE, 2017.
- [3] Jingyuan Chen, Lin Ma, Xinpeng Chen, Zequn Jie, and Jiebo Luo. Localizing natural language in videos. *AAAI*, 2019.
- [4] Shaoxiang Chen and Yu-Gang Jiang. Semantic proposal for activity localization in videos via sentence query. 2019.
- [5] Kevin Duarte, Yogesh S Rawat, and Mubarak Shah. Videocapsulenet: A simplified network for action detection. In *Advances in Neural Information Processing Systems*, 2018.
- [6] Kuncheng Fang, Lian Zhou, Cheng Jin, Yuejie Zhang, Kangnian Weng, Tao Zhang, and Weiguo Fan. Fully convolutional video captioning with coarse-to-fine and inherited attention. In *Proceedings of the AAAI Conference on Artificial Intelligence*, volume 33, pages 8271–8278, 2019.
- [7] Lianli Gao, Kaixuan Fan, Jingkuan Song, Xianglong Liu, Xing Xu, and Heng Tao Shen. Deliberate attention networks for image captioning. 2019.
- [8] Kirill Gavrilyuk, Amir Ghodrati, Zhenyang Li, and Cees GM Snoek. Actor and action video segmentation from a sentence. In *Proceedings of the IEEE Conference on Computer Vision and Pattern Recognition*, pages 5958–5966, 2018.
- [9] Dongliang He, Xiang Zhao, Jizhou Huang, Fu Li, Xiao Liu, and Shilei Wen. Read, watch, and move: Reinforcement learning for temporally grounding natural language descriptions in videos. 2019.
- [10] Geoffrey E Hinton, Alex Krizhevsky, and Sida D Wang. Transforming auto-encoders. In *International Conference on Artificial Neural Networks*, pages 44–51. Springer, 2011.
- [11] Geoffrey E Hinton, Sara Sabour, and Nicholas Frosst. Matrix capsules with EM routing. In *International Conference on Learning Representations*, 2018.
- [12] Ronghang Hu, Marcus Rohrbach, and Trevor Darrell. Segmentation from natural language expressions. In *European Conference on Computer Vision*, pages 108–124. Springer, 2016.
- [13] Hueihan Jhuang, Juergen Gall, Silvia Zuffi, Cordelia Schmid, and Michael J Black. Towards understanding action recognition. In *Computer Vision (ICCV), 2013 IEEE International Conference on*, pages 3192–3199. IEEE, 2013.
- [14] Will Kay, Joao Carreira, Karen Simonyan, Brian Zhang, Chloe Hillier, Sudheendra Vijayanarasimhan, Fabio Viola, Tim Green, Trevor Back, Paul Natsev, et al. The kinetics human action video dataset. *arXiv preprint arXiv:1705.06950*, 2017.
- [15] Sahar Kazemzadeh, Vicente Ordonez, Mark Matten, and Tamara Berg. Referitgame: Referring to objects in photographs of natural scenes. In *Proceedings of the 2014 conference on empirical methods in natural language processing (EMNLP)*, pages 787–798, 2014.
- [16] Diederik P Kingma and Jimmy Ba. Adam: A method for stochastic optimization. *arXiv preprint arXiv:1412.6980*, 2014.
- [17] Rodney LaLonde and Ulas Bagci. Capsules for object segmentation. *arXiv preprint arXiv:1804.04241*, 2018.
- [18] Yitong Li, Martin Renqiang Min, Dinghan Shen, David Carlson, and Lawrence Carin. Video generation from text. In *Thirty-Second AAAI Conference on Artificial Intelligence*, 2018.
- [19] Zhenyang Li, Ran Tao, Efstratios Gavves, Cees GM Snoek, Arnold WM Smeulders, et al. Tracking by natural language specification. In *CVPR*, volume 1, page 5, 2017.
- [20] Zhihui Li, Lina Yao, Xiaoqin Zhang, Xianzhi Wang, Salil Kanhere, and Huaxiang Zhang. Zero-shot object detection with textual descriptions. 2019.
- [21] Amir Mazaheri and Mubarak Shah. Visual text correction. In *The European Conference on Computer Vision (ECCV)*, September 2018.
- [22] Tomas Mikolov, Ilya Sutskever, Kai Chen, Greg S Corrado, and Jeff Dean. Distributed representations of words and phrases and their compositionality. In *Advances in neural information processing systems*, pages 3111–3119, 2013.
- [23] Adam Paszke, Sam Gross, Soumith Chintala, Gregory Chanan, Edward Yang, Zachary DeVito, Zeming Lin, Alban Desmaison, Luca Antiga, and Adam Lerer. Automatic differentiation in pytorch. 2017.
- [24] Sara Sabour, Nicholas Frosst, and Geoffrey E Hinton. Dynamic routing between capsules. In *Advances in Neural Information Processing Systems*, pages 3856–3866, 2017.
- [25] Hengcan Shi, Hongliang Li, Fanman Meng, and Qingbo Wu. Key-word-aware network for referring expression image segmentation. In *The European Conference on Computer Vision (ECCV)*, September 2018.
- [26] Gunnar A Sigurdsson, Gül Varol, Xiaolong Wang, Ali Farhadi, Ivan Laptev, and Abhinav Gupta. Hollywood in homes: Crowdsourcing data collection for activity understanding. In *European Conference on Computer Vision*, pages 510–526. Springer, 2016.
- [27] Weixuan Wang, Zhihong Chen, and Haifeng Hu. Hierarchical attention network for image captioning. In *Proceedings of the AAAI Conference on Artificial Intelligence*, volume 33, pages 8957–8964, 2019.
- [28] Chenliang Xu, Shao-Hang Hsieh, Caiming Xiong, and Jason J Corso. Can humans fly? action understanding with multiple classes of actors. In *Proceedings of the IEEE Conference on Computer Vision and Pattern Recognition*, pages 2264–2273, 2015.
- [29] Quanzeng You, Hailin Jin, Zhaowen Wang, Chen Fang, and Jiebo Luo. Image captioning with semantic attention. In *Proceedings of the IEEE conference on computer vision and pattern recognition*, pages 4651–4659, 2016.
- [30] Haonan Yu, Jiang Wang, Zhiheng Huang, Yi Yang, and Wei Xu. Video paragraph captioning using hierarchical recurrent neural networks. In *Proceedings of the IEEE conference on computer vision and pattern recognition*, pages 4584–4593, 2016.

- [31] Wei Zhao, Jianbo Ye, Min Yang, Zeyang Lei, Suofei Zhang, and Zhou Zhao. Investigating capsule networks with dynamic routing for text classification. *arXiv preprint arXiv:1804.00538*, 2018.
- [32] Yiyi Zhou, Rongrong Ji, Jinsong Su, Xiaoshuai Sun, and Weiqiu Chen. Dynamic capsule attention for visual question answering. 2019.